The Journal of Clinical Pharmacology
2025, 65(2) 160–169

DOI: 10.1002/jcph.6133

Determination of Vatiquinone Drug-Drug Interactions, as CYP450 Perpetrator and Victim, Using Physiologically Based Pharmacokinetic (PBPK) Modeling and Simulation

Lucy Lee, PharmD, FCP[1], Noriko Okudaira, PhD[2], Katsuyuki Murase, PhD[1], Ronald Kong, PhD[1], and Hannah M. Jones, PhD[2]

Abstract

Vatiquinone, a 15-lipoxygenase inhibitor, is in development for patients with Friedreich's ataxia. Physiologically based pharmacokinetic (PBPK) modeling addressed drug-drug interaction gaps without additional studies. A PBPK model (Simcyp Simulator version 21, full model) was developed using parameters obtained from in vitro studies, in silico estimation and optimization, and two clinical studies. A venous blood dosing model best characterized vatiquinone lymphatic absorption. Apparent oral clearance (CL/F) was used to optimize intrinsic clearance (CL_{int}). Intestinal availability (F_g) was estimated using the hybrid flow term (Q_{gut}), unbound fraction in the enterocytes (fu_{gut}), and gut intrinsic metabolic clearance ($CLu_{G,int}$). Renal clearance (CL_R) was set to zero. Assuming an F_a of 1, CYP3A4 contribution (fm_{CYP3A4}) was further optimized. The PBPK model was verified with two clinical studies and demonstrated that it adequately characterized vatiquinone PK. As a perpetrator, the model predicted no risk for vatiquinone to significantly alter the drug exposures of CYP3A4 and CYP1A2 substrates as evident bynegligible reduction in both midazolam and caffeine area under the curve $(AUC)_{inf}$ and C_{max}. As a victim, the model predicted that vatiquinone exposures are weakly influenced by moderate CYP3A4 inhibitors and inducers. With fluconazole coadministration, vatiquinone AUC_{inf} and C_{max} increased by nearly 50% and 25%, respectively. With efavirenz coadministration, vatiquinone AUC_{inf} and C_{max} decreased by approximately 20% and 10%, respectively. Results suggested that vatiquinone does not significantly impact CYP3A4 and CYP1A2 substrates and that moderate CYP3A4 inhibitors and inducers weakly impact vatiquinone AUC.

Keywords

drug-drug interaction, PBPK modeling, rare disease, vatiquinone

Introduction

Vatiquinone (PTC743, EPI-743, alpha-tocotrienol quinone) is an orally bioavailable small molecule being developed by PTC Therapeutics for the treatment of disorders characterized by high levels of oxidative stress and dysregulation of energy metabolism.[1] Vatiquinone is a potent inhibitor that prevents ferroptotic cell death by inhibiting 15-lipoxygenase (15-LO), a key enzyme in the ferroptosis pathway, and alleviates oxidative stress and lipid peroxidation, thereby preventing neuronal dysfunction and cell death. In patients with diseases characterized by oxidative stress, the activity of 15-LO is increased. This can lead to the depletion of glutathione (GSH) and other antioxidants.[2,3] Indeed, in diseases of the central nervous system, the role of 15-LO as a key enzyme in the biological process of ferroptosis has been shown.[4,5] Treatment with vatiquinone has been shown to improve disease symptoms and arrest or reverse disease progression by increasing GSH levels, thus decreasing the ratio of oxidized GSH to reduced GSH (OX/GSH).[6,7] Long-term improvement in neurological and neuromuscular function in patients with Friedreich's ataxia has been demonstrated clinically, and safety data suggest that vatiquinone is well tolerated with no dose-limiting toxicities.[8]

The pharmacokinetics (PK) and pharmacodynamics (PD) of vatiquinone were assessed in Phase 1 studies in healthy volunteers and Phase 2/2b studies in pediatric and adult patients, using an increase in GSH as a surrogate PD marker of 15-LO inhibition. To

[1]PTC Therapeutics, Inc., Warren, NJ, USA
[2]Certara UK Limited, Simcyp Division, Sheffield, UK

Submitted for publication 6 July 2024; accepted 26 August 2024.

Corresponding Author:
Lucy Lee, PharmD, FCP, PTC Therapeutics, Inc., Warren, NJ 07059
E-mail: llee@ptcbio.com

maximize potential clinical benefit, a dose was targeted that achieved PK exposures in which a near-complete decrease of the OX/GSH ratio was observed.

Since body weight correlates with drug clearance, a body weight-based dosing regimen was developed to allow patients across a broad age range to achieve consistent vatiquinone PK exposures. Human mass balance and metabolite identification study demonstrated that hepatic elimination is the main route of drug elimination. Following an oral dose of ^{14}C-vatiquinone in male subjects, mean cumulative recovery was 92.9% with 70.6% in feces and 22.3% in urine. Recovery of unchanged vatiquinone in feces was 6.77% of dose indicating near-complete absorption. No major metabolite was identified.[9]

Based on reaction phenotyping studies, vatiquinone metabolism was found to be mainly mediated by CYP3A4. Clinical studies demonstrated a lack of a clinically relevant effect of vatiquinone on CYP2C9, CYP2C19, and breast cancer resistance protein (BCRP) substrates.[10,11] Coadministration of 400 mg vatiquinone with 200 mg itraconazole (a strong CYP3A4 inhibitor) resulted in an increase in vatiquinone C_{max} and systemic exposure (area under the curve $[AUC]_{0\text{-inf}}$) by approximately 3.5-fold and 2.9-fold, respectively. Similarly, coadministration of 400 mg vatiquinone with 600 mg rifampicin (a strong CYP3A4 inducer) resulted in a decrease in vatiquinone C_{max} and $AUC_{0\text{-inf}}$ by approximately 36% and 46%, respectively.[12] The clinical relevance of strong CYP3A4 inhibitors and inducers will be determined with clinical safety and efficacy data and any exposure–response relationships.

Since vatiquinone is a vitamin E form, its absorption mechanism follows that of vitamin E. Vitamin E, as well as other lipophilic components such as fatty acids, cholesterol, and other liposoluble vitamins, is absorbed via lipid micelles in the small intestine. While in enterocytes, vitamin E is incorporated into chylomicrons, which pass into the lymphatic system and the circulation.[13,14] Consistent with this mechanism, the result of the food-effect study demonstrated significant enhancement of vatiquinone activity when administered with low-fat meals. Vatiquinone AUCs were 8-fold higher in subjects who consumed low-fat meals compared with subjects who fasted. Food, especially high-fat food, increases bile flow, which then aids the emulsification of the lipid (and vatiquinone) to form micelles, facilitating absorption through the enterocyte into the lymphatic system. Vatiquinone is orally administered either in capsule form or as a solution. It is recommended that patients take vatiquinone with low-fat meals that consist of at least 25% fat of the caloric content. With an estimated effective half-life ($t_{1/2}$) of approximately 9 h, a three times daily dosing (TID) regimen is required to maintain therapeutic drug exposures.

Two drug-drug interaction (DDI) studies were conducted clinically; however, a few DDI questions remained to be clarified. To address the further DDI questions during the development of vatiquinone, the use of physiologically based pharmacokinetic (PBPK) modeling was discussed. As such, a virtual approach was taken to address these questions. This approach was feasible because adequate clinical PK data are available to support reliable models that sufficiently characterize the absorption, distribution, metabolism, and elimination of vatiquinone. Since vatiquinone is a vitamin E form, its PK are thought to be best described by a direct venous dosing model that characterizes a drug where the absorption is predominately via the lymphatic route. PBPK modeling predicted the outcome of vatiquinone DDIs both as a perpetrator and victim. As a perpetrator, in vitro data suggested vatiquinone was a borderline potential inducer of CYP3A4 and CYP1A2. PBPK modeling predicted the negligible impact of administering vatiquinone with CYP3A4 and CYP1A2 substrates. As a victim, it was of interest to evaluate vatiquinone exposures when coadministered with moderate and/or weak CYP3A4 inhibitors and inducers, especially since itraconazole and rifampicin demonstrated positive effects. PBPK modeling also predicted negligible to low impact of administering vatiquinone with moderate CYP3A4 inhibitors and inducers. The current study demonstrated the use of PBPK modeling to potentially avoid the need of additional clinical studies to address the DDI gaps.

Methods

Institutional review board (IRB)/ethics and informed consent do not apply since this is a pooled data analysis across several studies.

Modeling Strategy

As shown in Figure 1, there were three parts to the modeling strategy: (1) model development, (2) model verification, and (3) model application. The Simcyp Population-Based Simulator Version 21 was used for all PBPK modeling and simulation. The data that were used in each part are listed.

Model Development

PBPK models that simulate vatiquinone PK in the fed state were developed using in vitro studies, in silico estimation and optimization, and two clinical studies. The two clinical studies were a DDI study (itraconazole) and a human mass balance study. Two models, the oral absorption model and venous blood dosing model were developed using the Simcyp Simulator (version 21). The latter mimics the absorption via the

Figure 1. Schematic of PBPK modeling strategy.

lymphatic route. In the oral absorption model, the full PBPK with first-order absorption model was used. The fraction of vatiquinone absorbed (F_a) was assumed to be 1 since the human mass balance study data indicated near-complete absorption of vatiquinone. Intestinal availability (F_g) was estimated using the hybrid flow term (Q_{gut}), unbound fraction in the enterocytes (fu_{Gut}), and the intrinsic metabolic clearance in the gut ($CLu_{G,int}$). In the venous blood dosing model, the drug enters the venous bloodstream without intestinal and hepatic first-pass metabolism, which mimics the lymphatic absorption. In each model, intrinsic clearance (CL_{int}) was optimized to recover the apparent oral clearance (CL/F) of 94.3 L/h obtained from healthy volunteer studies. CL/F was calculated using $AUC_{0\text{-inf}}$ after administration of vatiquinone in the absence of itraconazole.

Renal clearance (CL_R) was set to zero since unchanged vatiquinone was not detected in urine. The data from DDI study with itraconazole were used to assign the relative contribution of CYP3A4 for drug clearance. The maximal fold induction (Ind_{max}) and half maximal fold induction ($IndC_{50}$) for CYP3A4 induction were incorporated within the PBPK model. Metabolism by enzymes other than CYP3A4 was lumped into "additional" intrinsic clearance. A Log P value that predicts the observed unbound fraction (fu) (0.022) was used since Log P was not measurable. The predicted blood:plasma ratio was used.

Model Verification

The contribution of CYP3A4 to the overall clearance of vatiquinone was verified using data from two studies, one DDI study (rifampicin) and one Phase 2 patient study. CYP3A4 induction parameters were evaluated by comparison of the simulated vatiquinone plasma concentration–time profiles (visual check) and PK parameters after multiple dosing to observed data. Observed data were summarized following single and repeat dosing. The model was further verified using clinical PK data after multiple dosing of 200 mg TID and 400 mg TID in patients with Friedreich's ataxia. Predictions were considered to be reasonably accurate if the exposures were within 1.5-fold of the observed data.

Model Application

PBPK simulations were performed for DDI scenarios after satisfactory model verifications.

As a perpetrator:

- Prediction of plasma concentrations of midazolam following a single oral dose of 5 mg administered in the absence of vatiquinone and on the 12th day of 14 days of dosing with vatiquinone (400 mg TID; 9:00, 15:00, 21:00) in healthy subjects.
- Prediction of plasma concentrations of caffeine following a single oral dose of 150 mg administered in the absence of vatiquinone and on the 12th day of 14

days of dosing with vatiquinone (400 mg TID; 9:00, 15:00, 21:00) in healthy subjects.

As a victim:

- Simulation of plasma concentrations of vatiquinone in healthy subjects following a single oral dose of 400 mg administered in the absence of fluconazole and on the 5th day of 6 days of dosing with fluconazole (400 mg once daily (QD) on Day 1 and 200 mg QD from Day 2 to Day 6).
- Simulation of plasma concentrations of vatiquinone in healthy subjects following a single oral dose of 400 mg administered in the absence of efavirenz and on the 14th day of 15 days of dosing with 600 mg efavirenz QD.

Results

Model Development

Table 1 lists the final input parameters for the oral absorption model and venous blood dosing model.

Both models reproduced the clinical PK data used for the model development. The optimized vatiquinone CL_{int} and fm_{CYP3A4} were 1260 μL/min/mg protein and 0.7, respectively, in the oral absorption model, and 4000 μL/min/mg protein and 0.95, respectively, in the venous blood dosing model. The K_p scalar was optimized in each model to describe the overall plasma concentration–time profiles. The simulated profile of vatiquinone using the venous blood dosing model is shown in Figure 2. Table 2 lists the simulated and observed geometric mean $AUC_{0\text{-inf}}$ and C_{max} values and corresponding geometric mean ratios (GMRs) for vatiquinone in the absence and presence of itraconazole. The simulated profiles of vatiquinone were generally comparable to the clinical data, but the simulated peak concentrations in the presence of itraconazole were lower than the observed values. The simulated geometric mean $AUC_{0\text{-inf}}$ ratio for vatiquinone in the presence of itraconazole was within 1.25-fold of the observed value, but the C_{max} ratio was lower than the observed value by >2-fold.

Model Verification

The final models were verified by comparison of simulations to the results of two clinical studies. The two studies were the DDI study and the Phase 2 Friedreich's ataxia study. The actual data from these two studies along with the simulated results are provided in Table 3 (PK parameters) and Figure 3 (PK concentration–time profiles), although the simulated inter-individual variability was lower than the observed data.

The oral absorption model reasonably recovered the observed PK data after single and multiple dosing but significantly overestimated the DDI study with rifampicin. To recover the geometric $AUC_{0\text{-inf}}$ ratio, fm_{CYP3A4} had to be reduced from 0.7 to 0.3 (data not shown). In the base model, the in vitro fm_{CYP3A4} (0.432) was used. The in vivo fm_{CYP3A4} was modified to 0.7 to recover the observed AUC ratio in the absence and presence of itraconazole. However, to describe the rifampicin clinical data, an in vivo fm_{CYP3A4} of 0.3 was required. Using the venous blood dosing model, the simulated concentration profiles of vatiquinone alone and in combination with rifampicin are comparable to the clinical data (Figure 3, Panel a). The simulated geometric mean $AUC_{0\text{-inf}}$, C_{max}, and t_{max} (not shown) were within 1.25-fold of the clinical data (Table 3, top). Although the model underpredicted the drug interaction with rifampicin, the simulated $AUC_{0\text{-inf}}$ and C_{max} GMRs were within 1.5-fold of the observed data. For the Phase 2 Friedreich's ataxia study, the simulated multiple dose data were comparable to the clinical data for both 200 and 400 mg doses and for both Day 1 and Day 91 (Figure 3, Panel b). The simulated geometric C_{max} and $AUC_{0\text{-24 h}}$ on Day 1 and Day 91 were within 1.5-fold of the clinical data (Table 3, bottom).

Model Application

The venous blood dosing model was selected to predict victim and perpetrator DDIs because the model reasonably recovered the observed DDI studies both with itraconazole and rifampicin. The mean simulated $AUC_{0\text{-72 h}}$ and C_{max} for midazolam and caffeine, sensitive CYP3A4 and CYP1A2 substrates, respectively, when administered alone and in combination with 14 days of vatiquinone dosing are shown in Table 4 (top). The mean simulated AUC_{inf} and C_{max} for vatiquinone when administered alone and in combination with 14 days of dosing with the moderate CYP3A4 inducer, fluconazole and efavirenz, respectively, are shown in Table 4 (bottom). Geometric mean, GMRs, and 90% confidence intervals (CIs) are also listed. The risk for each DDI scenario is summarized in Table 5.

As a perpetrator, there is no risk for vatiquinone to significantly alter the drug exposures of CYP3A4 and CYP1A2 substrates. There is negligible reduction in midazolam AUC_{inf} (GMR: 0.995; 90% CI [0.994, 0.996]) and C_{max} (GMR: 0.997; 90% CI [0.997, 0.998]). There is also negligible reduction in caffeine AUC_{inf} (GMR: 0.911; 90% CI [0.891, 0.932]) and C_{max} (GMR: 0.979; 90% CI [0.974, 0.985]). As a victim, vatiquinone exposures are weakly influenced by moderate CYP3A4 inhibitors and inducers. With coadministration of fluconazole, vatiquinone AUC_{inf} and C_{max} increased by less than 50% and 25%, respectively. The corresponding GMRs are 1.48 (90% CI [1.45, 1.51]) and 1.24 (90% CI [1.23, 1.25]), respectively. With coadministration of efavirenz, vatiquinone AUC_{inf} and C_{max} decreased by

Table 1. Final Input Parameters for the PBPK Model

Parameter	Value	Comments
Physiochemical properties		
Molecular weight (g/mol)	440.66	
Log P	4.8	Optimized to recover fu
Compound type	Neutral	
pKa	Not applicable	
B:P	1.36	Predicted
fu	0.0220	
Main binding protein	HSA	Assumed
Absorption (first-order model)		
fu_{gut}	0.000133	Predicted
$P_{eff,man}$ (pred) ($\times 10^{-4}$ cm/s)	3	Optimized to recover ka
Q_{gut} (L/h)	12.4	Predicted
Fa	1.00	Assumed
ka (1/h)	1.27	Clinical study
t_{lag} (h)	3.67	
F_G	1.00	Estimated within Simcyp
Distribution (full PBPK model) V_{SS} (L/kg)		
Oral absorption	3.39	Method 1[21]
Venous blood dosing K_P scalar	4.49	Method 1[14]
Oral absorption	0.3	Optimized
Venous blood dosing	0.4	Optimized
Elimination		
CL/F (L/h)	94.3	Clinical study
fm_{CYP3A4}		
Oral absorption	0.7	Clinical study, optimized
Venous blood dosing	0.95	Clinical study, optimized
CYP3A4 CL_{int} (µL/min/mg)		
Oral absorption	882	Retrograde model. CL/F obtained from Clinical study (94.3 L/h); fm_{CYP3A4} 0.7
Additional HLM CL_{int} (µL/min/mg)	378	
CYP3A4 CL_{int} (µL/min/mg)		
Venous blood dosing	3800	Retrograde model. CL/F obtained from Clinical study (94.3 L/h); fm_{CYP3A4} 0.95
Additional HLM CL_{int} (µL/min/mg)	200	
fu_{mic}	1	
CL_R (L/h)	0	Clinical study
Drug-drug interaction		
CYP3A4 Ind_{max}	4.26	Scaled using rifampicin data. The same values were applied to CYP3A5 to simulate DDI with rifampicin
CYP3A4 $IndC_{50}$ (µM)	3.70	
CYP1A2 Ind_{max}	2.61	In vitro study
CYP1A2 $IndC_{50}$ (µM)	1.80	
CYP1A2 Ind_{max}	1.04	Scaled using omeprazole data
CYP1A2 $IndC_{50}$ (µM)	0.0193	
fu_{inc}	0.152	Predicted, Austin et al (2005),[22] Kilford et al (2008)[23]

B:P, blood to plasma ratio; CL/F, human oral clearance; CL_{int}, intrinsic metabolic clearance; CL_R, human renal clearance; CYP, cytochrome P450; F_a, fraction of dose absorbed; F_g, prediction of intestinal availability; fm_{CYP3A4}, fraction metabolized by CYP3A4; DDI, drug-drug interaction; fu, unbound fraction in plasma; fu_{gut}, unbound fraction in the gut; fu_{inc}, unbound fraction in incubation; fu_{mic}, unbound fraction in microsomes; HLM, human liver microsome; $IndC_{50}$, half-maximal induction; Ind_{max}, maximum fold induction; ka, first-order absorption rate; K_P, plasma partition coefficient; PBPK, physiologically based pharmacokinetic; $P_{eff,man}$, effective permeability predicted in human; pKa, acid dissociation constant; Q_{gut}, hybrid flow term; t_{lag}, lag time; V_{SS}, volume of distribution.

approximately 20% and 10%, respectively. The corresponding GMRs are 0.786 (90% CI [0.773, 0.800]) and 0.866 (90% CI [0.857, 0.874]), respectively.

Discussion And Conclusions

Recently, an increasing number of drug development programs have utilized PBPK modeling and simulation to facilitate the predictions of human drug PK without the need for conducting additional clinical studies. The utility of PBPK modeling and simulation has evolved with its applicability at all stages of drug development and regulatory review.[15] During regulatory review of new drug and biologics license applications, questions are routinely asked about how intrinsic factors (e.g., organ dysfunction, age, and genetics) and extrinsic factors (e.g., DDIs) might influence exposure–response relationships and the impact of these individual factors

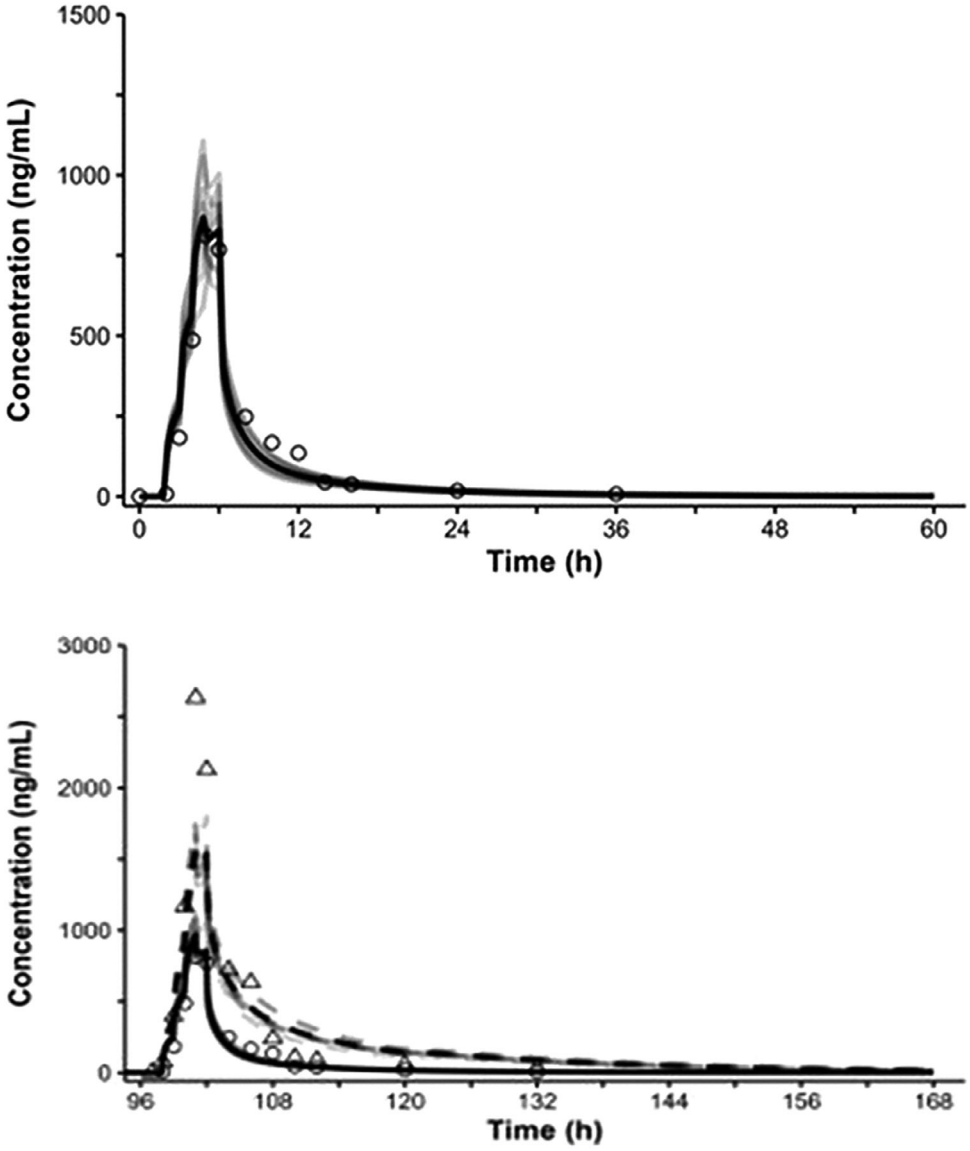

Figure 2. Simulated and observed vatiquinone concentration–time profiles after single oral dose of 400 mg vatiquinone (top) and in combination with itraconazole (bottom) in healthy subjects.

on the efficacy and safety of the candidate compound. PBPK modeling and simulation is one of the tools that can be used to virtually address these critical questions.[16–19]

As a perpetrator, clinical doses of vatiquinone did not have a significant impact on the drug exposures of tolbutamide (CYP2C9 substrate), omeprazole (CYP2C19 substrate), and rosuvastatin (BCRP substrate). Although it was not anticipated that vatiquinone would have any induction effects on CYP3A4 and CYP1A2 substrates, PBPK modeling and simulation was used to rule out any positive effect in light of a marginally positive in vitro induction study result. As a victim, in the presence of itraconazole, a strong CYP3A4 inhibitor, vatiquinone C_{max} and $AUC_{0\text{-inf}}$ increased by approximately 245% and 188%, respectively. In the presence of rifampicin, a strong CYP3A4 inducer, vatiquinone C_{max} and $AUC_{0\text{-inf}}$ decreased by approximately 36% and 46%, respectively. Based on target patient population, it was of further interest to understand the influence of moderate CYP3A4 inhibitors and inducers on vatiquinone drug exposure.

As mentioned, vatiquinone is a vitamin E form. It is known that vitamin E is incorporated in mixed micelles and absorbed by enterocytes.[20] In lymphatic absorption, it was assumed that first-pass metabolism is negligible, and orally administered drug molecules enter the systemic circulation without pre-systemic loss. Lymphatic absorption is a component of various highly

Table 2. Simulated and Observed Geometric Mean $AUC_{0\text{-inf}}$ and C_{max} and Corresponding GMRs for Vatiquinone in Healthy Volunteers (Venous Blood Dosing Model)

	Vatiquinone (400 mg)		Vatiquinone + Itraconazole (5 days TID, 200 mg)		GMR	
	$AUC_{0\text{-inf}}$ (h•ng/mL)	C_{max} (ng/mL)	$AUC_{0\text{-inf}}$ (h•ng/mL)	C_{max} (ng/mL)	$AUC_{0\text{-inf}}$	C_{max}
Simulated	3981	1187	11,393	1873	2.86	1.58
CV%	23.9	28.9	59.4	30.5	41.5	11
90% CI—Lower	3880	1150	10,731	1813	2.74	1.56
90% CI—Upper	4085	1224	12,096	1935	2.99	1.6
Observed	3910	992	11,300	3430	2.89	3.45
S/O	1.02	1.20	1.01	0.546	0.990	0.458

CI, confidence interval; CV, coefficient of variation; GMR, geometric mean ratio; S/O, simulated/observed; TID, three times a day.

Table 3. Model Verification of Venous Blood Dosing Model—PK Parameters

	Vatiquinone (400 mg)		Vatiquinone + Rifampicin (14 days TID, 600 mg)		GMR	
	$AUC_{0\text{-inf}}$* (h•ng/mL)	C_{max} (ng/mL)	$AUC_{0\text{-inf}}$* (h•ng/mL)	C_{max} (ng/mL)	$AUC_{0\text{-inf}}$*	C_{max}
Simulated	3795	1094	2852	920	0.752	0.841
CV%	25.6	29.1	21.5	28.6	11.7	6.55
90% CI—Lower	3692	1061	2786	892	0.742	0.835
90% CI—Upper	3900	1129	2919	948	0.761	0.847
Observed	3420	973	1830	619	0.539	0.636
S/O	1.11	1.12	1.56	1.49	1.39	1.32

		Day 1		Day 91	
Dose	$AUC_{0\text{-8 h}}$ (h•ng/mL)	C_{max} (ng/mL)	$AUC_{0\text{-8 h}}$ (h•ng/mL)	C_{max} (ng/mL)	
200 mg TID	Simulated	1433	554	1881	599
	Observed	1026	466	1949	689
	S/O	1.40	1.19	0.965	0.870
400 mg TID	Simulated	2829	1092	3710	1180
	Observed	2428	1019	3494	905
	S/O	1.17	1.07	1.06	1.30

CI, confidence interval; CV, coefficient of variation; GMR, geometric mean ratio; PK, pharmacokinetic; S/O, simulated/observed; TID, three times a day.

*Simulated $AUC_{0\text{-72 h}}$.

Top: Drug-drug interaction study: Simulated and observed geometric mean vatiquinone $AUC_{0\text{-inf}}$ and C_{max} in healthy volunteers.

Bottom: Phase 2 Friedreich's ataxia study: Simulated and observed geometric mean vatiquinone $AUC_{0\text{-8 h}}$ and C_{max} in patients with Friedreich's ataxia.

lipophilic drugs, but the fraction of dose absorbed via lymph varies for each drug, formulation, and dose. This remains one of the limitations of this venous dosing model. It is still challenging to quantitatively predict the contribution of the lymphatic route because the methods used to predict some parameters that govern the partition of drugs into intestinal lymph have not been established.

To overcome this limitation, both oral absorption and venous blood dosing models were evaluated during model development. Since both mechanisms contribute to vatiquinone absorption, prediction using either the oral absorption model or the venous blood dosing model alone could potentially overestimate or underestimate the impact on the concentrations of the victim drugs, respectively. The oral absorption model assumes 100% absorption via the portal vein. Due to the first-pass metabolism, CL_{int} required to recover the observed AUC is higher, and thus a stronger impact on victim drug is predicted in the presence of CYP3A inhibitors and inducers. The venous dosing model assumes 100% absorption via the lymphatic route. This requires a lower CL_{int} to recover the observed AUC and predicts a lesser impact on the victim drug. As a result, the predicted fm_{CYP3A} values were higher in the venous dosing model.

The venous blood dosing model recovered the AUC ratio in the presence and absence of itraconazole, but the C_{max} ratio was underestimated (Table 2, Figure 2). Considering the near-complete absorption, further

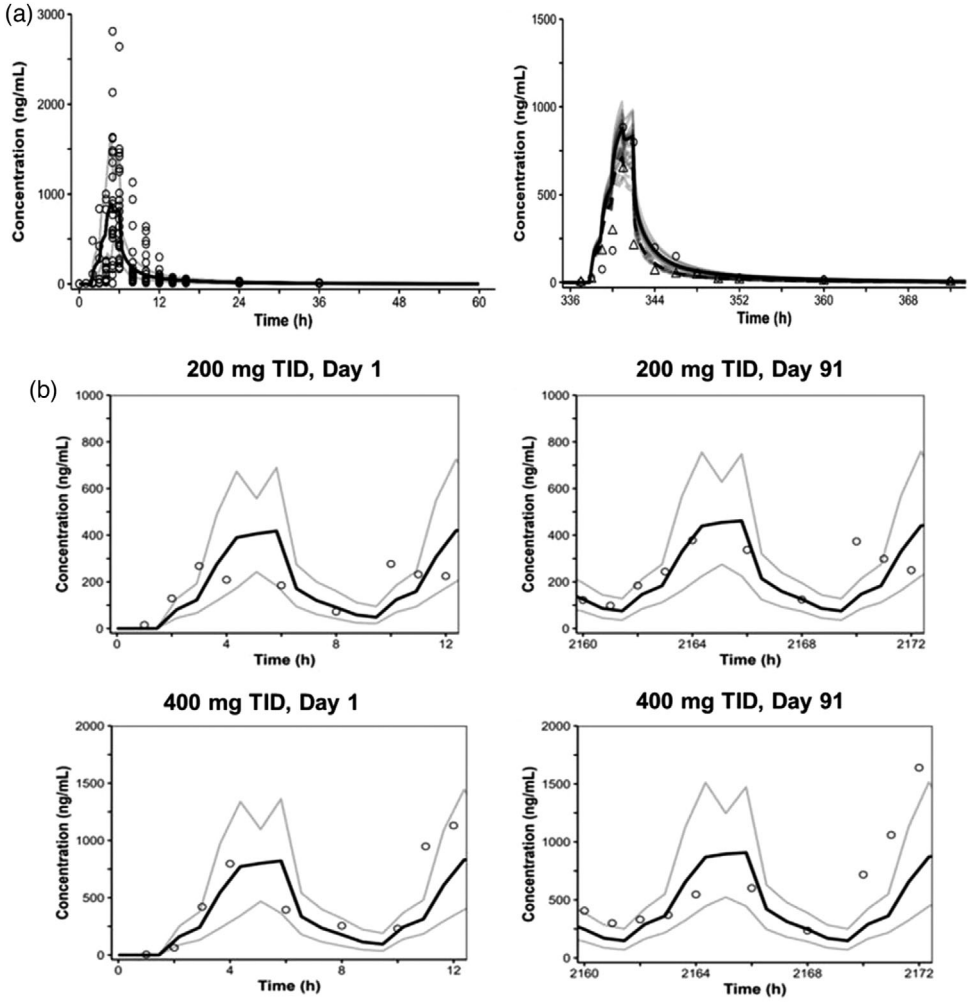

Figure 3. Model verification of venous blood dosing model—PK concentration–time profiles.

increase in Fa by itraconazole is unlikely, thus the increase in AUC represents the inhibition of elimination. A possible mechanism of C_{max} change is the inhibition of intestinal P-gp and BCRP by itraconazole, which increases the absorption rate. Vectorial transport of vatiquinone across P-gp or BCRP-expressing cell lines but due to the low solubility and high adsorption, conclusive results have not been obtained whether vatiquinone is a substrate of P-gp or BCRP.

The contribution of lymphatic absorption of 0% and 100% corresponds to the oral absorption model and venous blood dosing model, respectively. The higher contribution of the lymph route reduces the first-pass metabolism and increases the plasma exposure of the drug in addition to the lesser impact on victim drug. The true AUC ratio could fall between the two models and supports the understanding of the predicted victim DDI using the two models. Due to the assumption of negligible first-pass metabolism in the venous blood dosing model, DDI with rifampicin may be underpredicted (Table 3) despite the high metabolic CL_{int} values. On the other hand, DDI with rifampicin was overpredicted. Underprediction of the C_{max} ratio in the DDI study with itraconazole (Table 2) may also be partially explained by the lack of inhibition of first-pass metabolism in the venous blood dosing model. This simulation also suggests that if fm_{CYP3A4} is determined correctly in the in vitro experiments or in the in vivo metabolite identification studies, contribution of lymphatic absorption can possibly be determined using the DDI study results. Of the two models, the venous blood dosing model was selected because the lymphatic route is known to be the main absorption pathway for vitamin E and its forms such as vatiquinone. Further, the venous blood dosing model fits well with the clinical drug-drug data as demonstrated during model verification.

In conclusion, PBPK modeling facilitated the need for addressing vatiquinone DDI gaps without the need

Table 4. Simulated Geometric Mean Vatiquinone AUC and C_{max} and Corresponding GMRs for Drug-Drug Interaction Scenarios as Perpetrator (Top) and Victim (Bottom) (Venous Blood Dosing Model)

Sensitive CYP3A4 Substrate	Midazolam (5 mg)		Vatiquinone + Midazolam		GMR	
	$AUC_{0\text{-}72\ h}$ (h•ng/mL)	C_{max} (ng/mL)	$AUC_{0\text{-}72\ h}$ (h•ng/mL)	C_{max} (ng/mL)	$AUC_{0\text{-}72\ h}$	C_{max}
Geometric mean	65.6	25.3	65.3	25.2	0.995	0.997
90% CI—lower	58.2	22.8	57.9	22.8	0.994	0.997
90% CI—upper	74.0	28.0	73.6	27.9	0.996	0.998
Sensitive CYP1A2 Substrate	**Caffeine (150 mg)**		**Vatiquinone + Caffeine**		**GMR**	
	$AUC_{0\text{-}72\ h}$ (h•ng/mL)	C_{max} (ng/mL)	$AUC_{0\text{-}72\ h}$ (h•ng/mL)	C_{max} (ng/mL)	$AUC_{0\text{-}72\ h}$	C_{max}
Geometric mean	25,442	3507	23,187	3435	0.911	0.979
90% CI–lower	22,877	3356	20,792	3285	0.891	0.974
90% CI–upper	28,295	3666	25,860	3592	0.932	0.985
Moderate CYP3A4 Inhibitor	**Vatiquinone (400 mg)**		**Vatiquinone + Fluconazole**		**GMR**	
	$AUC_{0\text{-}inf}$ (h•ng/mL)	C_{max} (ng/mL)	$AUC_{0\text{-}inf}$ (h•ng/mL)	C_{max} (ng/mL)	$AUC_{0\text{-}inf}$	C_{max}
Geometric mean	3900	1154	5785	1426	1.48	1.24
90% CI–lower	3737	1098	5475	1357	1.45	1.23
90% CI–upper	4069	1212	6113	1498	1.51	1.25
Moderate CYP3A4 Inducer	**Vatiquinone (400 mg)**		**Vatiquinone + Efavirenz**		**GMR**	
	$AUC_{0\text{-}inf}$ (h•ng/mL)	C_{max} (ng/mL)	$AUC_{0\text{-}inf}$ (h•ng/mL)	C_{max} (ng/mL)	$AUC_{0\text{-}inf}$	C_{max}
Geometric mean	3844	1113	3023	963	0.786	0.866
90% CI–lower	3669	1058	2906	916	0.773	0.857
90% CI–upper	4028	1170	3145	1012	0.800	0.874

CI, confidence interval; CYP, cytochrome P450; DDI, drug-drug interaction; GMR, geometric mean ratio.

Table 5. Vatiquinone Drug-Drug Interaction Risks as Perpetrator and Victim (Venous Blood Dosing Model)

Vatiquinone as Perpetrator	Category	$AUC_{0\text{-}inf}$ GMR	C_{max} GMR	DDI Risk*
Midazolam (5 mg QD)	Sensitive CYP3A4 substrate	0.995 [0.994-0.996]	0.997 [0.997-0.998]	No risk
Caffeine (150 mg QD)	Sensitive CYP1A2 substrate	0.911 [0.891-0.932]	0.979 [0.974-0.985]	No risk
Vatiquinone as Victim	**Category**	**$AUC_{0\text{-}inf}$ GMR**	**C_{max} GMR**	**DDI Risk***
Fluconazole (200 mg QD)	Moderate CYP3A4 inhibitor	1.48 [1.45-1.51]	1.24 [1.23-1.25]	Weak inhibition
Efavirenz (600 mg QD)	Moderate CYP3A4 inducer	0.786 [0.773-0.800]	0.866 [0.857-0.874]	Weak induction

CYP, cytochrome P450; DDI, drug-drug interaction; GMR, geometric mean ratio; TID, three times a day.

Top: Simulated geometric mean midazolam and caffeine AUC and C_{max} ratios, in the absence and presence of 400 mg vatiquinone TID in healthy subjects.

Bottom: Simulated geometric mean vatiquinone AUC and C_{max} ratios in the absence and presence of moderate CYP3A4 inhibitors and inducers in healthy subjects.

*No risk: AUC GMR $>$ 0.8 to $<$ 1.25; weak inhibition: AUC GMR $\geq$1.25-fold to $<$2-fold; weak induction: AUC GMR decreased by $\geq$20% to $<$50%; moderate induction: AUC GMR decreased by $\geq$50% to $<$80%.

for conducting additional studies. As a perpetrator, the simulations clearly demonstrate that there was no risk for vatiquinone to significantly alter the drug exposures of sensitive CYP3A4 (midazolam) and CYP1A2 (caffeine) substrates. As a victim, vatiquinone exposures were weakly influenced by moderate CYP3A4 inhibitor (fluconazole) and inducer (efavirenz). With moderate inhibitors, vatiquinone AUC_{inf} and C_{max} increased by less than 50% and 25%, respectively. With moderate inducers, vatiquinone AUC_{inf} and C_{max} minimally decreased by approximately 20% and 10%, respectively. Considering the wide therapeutic

window for vatiquinone, it is unlikely that moderate CYP3A4 inhibitors and inducers will have any clinically significant effect on the safety and efficacy of vatiquinone.

Acknowledgments

The authors thank Dr. Martin Thoolen for his scientific support on this project. The authors also thank Rosemary Barrett and Joe Yang for the editorial support.

Conflicts of Interest

This study is funded by PTC Therapeutics, Inc. All authors are employed by PTC Therapeutics, have received salary compensation for time and effort, and hold financial interest in the company.

Funding

This work was funded by PTC Therapeutics, Inc.

Data Availability Statement

The data that support the findings of this study are available from the corresponding author, LL, upon reasonable request.

References

1. Enns GM, Kinsman SL, Perlman SL, et al. Initial experience in the treatment of inherited mitochondrial disease with EPI-743. *Mol Genet Metab*. 2012;105(1):91-102.
2. Riederer P, Sofic E, Rausch WD, et al. Transition metals, ferritin, glutathione, and ascorbic acid in Parkinsonian brains. *J Neurochem*. 1989;52(2):515-520.
3. Piemonte F, Pastore A, Tozzi G, et al. Glutathione in blood of patients with Friedreich's ataxia. *Eur J Clin Invest*. 2001;31(11):1007-1011.
4. Joshi YB, Giannopoulos PF, Praticò D. The 12/15-lipoxygenase as an emerging therapeutic target for Alzheimer's disease. *Trends Pharmacol Sci*. 2015;36(3):181-186.
5. Guiney SJ, Adlard PA, Bush AI, Finkelstein DI, Ayton S. Ferroptosis and cell death mechanisms in Parkinson's disease. *Neurochem Int*. 2017; 104:34-48.
6. Blankenberg FG, Kinsman SL, Cohen BH, et al. Brain uptake of Tc99m-HMPAO correlates with clinical response to the novel redox modulating agent EPI-743 in patients with mitochondrial disease. *Mol Genet Metab*. 2012;107(4):690-699.
7. Pastore A, Petrillo S, Tozzi G, et al. Glutathione: a redox signature in monitoring EPI-743 therapy in children with mitochondrial encephalomyopathies. *Mol Genet Metab*. 2013;109(2):208-214.
8. Zesiewicz T, Salemi JL, Perlman S, et al. Double-blind, randomized, and controlled trial of EPI-743 in Friedreich's ataxia. *Neurodegener Dis Manag*. 2018;8(4):233-242.
9. Ma J, Lee L, Yao B, et al. Absorption, distribution, metabolism and excretion of ^{14}C-vatiquinone in rats, dogs, and human subjects. *Xenobiotica*. 2023;53(5):396-411.
10. Murase K, Lee L, Ma J, Barrett R, Thoolen M. Evaluation of vatiquinone drug-drug interaction potential in vitro and in a phase 1 clinical study with tolbutamide, a CYP2C9 substrate, and omeprazole, a CYP2C19 substrate, in healthy subjects. *Eur J Clin Pharmacol*. 2022;78(11):1823-1831.
11. Lee L, Murase K, Ma J, Thoolen M. Clinical drug-drug interaction between vatiquinone, a 15-lipoxygenase inhibitor, and rosuvastatin, a breast cancer resistance protein substrate. *Clin Pharmacol Drug Dev*. 2023;12(3):279-286.
12. Lee L, Thoolen M, Ma J, Kaushik D, Golden L, Kong R. Effect of Itraconazole, a CYP3A4 Inhibitor, and Rifampin, a CYP3A4 Inducer, on the Pharmacokinetics of Vatiquinone. *Clin Pharmacol Drug Dev*. 2024;13(12):1283-1290. doi:10.1002/cpdd.1461
13. Gagné A, Wei SQ, Fraser WD, Julien P. Absorption, transport, and bioavailability of vitamin E and its role in pregnant women. *J Obstet Gynaecol Can*. 2009;31(3):210-7.
14. Reboul E. Vitamin E bioavailability: mechanisms of intestinal absorption in the spotlight. *Antioxidants*. 2017;6(4):95.
15. Rowland M, Peck C, Tucker G. Physiologically-based pharmacokinetics in drug development and regulatory science. *Annu Rev Pharmacol Toxicol*. 2011;51:45-73. doi:10.1146/annurev-pharmtox-010510-100540
16. Huang SM, Rowland M. The role of physiologically based pharmacokinetic modeling in regulatory review. *Clin Pharmacol Ther*. 2012;91(3):542-549. doi:10.1038/clpt.2011.320
17. Zhao P, Zhang L, Grillo JA, et al. Applications of physiologically based pharmacokinetic (PBPK) modeling and simulation during regulatory review. *Clin Pharmacol Ther*. 2011;89(2):259-267. doi:10.1038/clpt.2010.298
18. Zhao P, Rowland M, Huang SM. Best practice in the use of physiologically based pharmacokinetic modeling and simulation to address clinical pharmacology regulatory questions. *Clin Pharmacol Ther*. 2012;92(1):17-20. doi:10.1038/clpt.2012.68
19. Huang SM. PBPK as a tool in regulatory review. *Biopharm Drug Dispos*. 2012;33(2):51-52. doi:10.1002/bdd.1777
20. Cohn W, Gross P, Grun H, Loechleiter F, Muller DPR, Zulauf M. Tocopherol transport and absorption. *Proc Nutr Soc*. 1992;51(2):179-188. doi:10.1079/PNS19920028
21. Poulin P, Theil FP. Prediction of pharmacokinetics prior to in vivo studies. 1. Mechanism-based prediction of volume of distribution. *J Pharm Sci*. 2002;91:129-156.
22. Austin RP, Barton P, Mohmed S, Riley RJ. The binding of drugs to hepatocytes and its relationship to physicochemical properties. *Drug Metab Dispos*. 2005;33:419-425.
23. Kilford PJ, Gertz M, Houston JB, Galetin A. Hepatocellular binding of drugs: correction for unbound fraction in hepatocyte incubations using microsomal binding or drug lipophilicity data. *Drug Metab Dispos*. 2008;36:1194-1197.